The Journal of Neuroscience, May 1, 1997, 17(9):3002–3013

Preferential Interaction of ω-Conotoxins with Inactivated N-type Ca^{2+} Channels

Jonathan W. Stocker,[1] Laszlo Nadasdi,[2] Richard W. Aldrich,[3] and Richard W. Tsien[1]

[1]Department of Molecular and Cellular Physiology and [2]Howard Hughes Medical Institute, Stanford University, Stanford, California 94305 and [3]Neurex Corporation, Menlo Park, California 94025

The selective block of N-type Ca^{2+} channels by ω-conotoxins has been a hallmark of these channels, critical in delineating their biological roles and molecular characteristics. Here we report that the ω-conotoxin-channel interaction depends strongly on channel gating. N-type channels (α_{1B}, α_2, and β_1) expressed in *Xenopus* oocytes were blocked with a variety of ω-conotoxins, including ω-CTx-GVIA, ω-CTx-MVIIA, and SNX-331, a derivative of ω-CTx-MVIIC. Changes in holding potential (HP) markedly altered the severity of toxin block and the kinetics of its onset and removal. Notably, strong hyperpolarization renders ω-conotoxin block completely reversible. These effects could be accounted for by a modulated receptor model, in which toxin dissociation from the inactivated state is ~60-fold slower than from the resting state. Because ω-conotoxins act exclusively outside cells, our results suggest that voltage-dependent inactivation of Ca^{2+} channels must be associated with an externally detectable conformational change.

Key words: calcium channel; ω-conotoxin; inactivation; voltage-dependent binding; modulated receptor hypothesis; N-type

Specific interactions between peptide neurotoxins and voltage-gated channels have been valuable in defining the contributions of various channels to key physiological processes. For example, the ω-conotoxins ω-CTx-GVIA and ω-CTx-MVIIA potently block N-type Ca^{2+} channels (Kasai et al., 1987; McCleskey et al., 1987; Plummer et al., 1989; Regan et al., 1991) and have been critical for their biochemical isolation (McEnery et al., 1991; Sakamoto and Campbell, 1991) and delineation of their diverse functional roles (Nowycky et al., 1985; Hirning et al., 1988; Stanley and Goping, 1991; Komuro and Rakic, 1992; Wheeler et al., 1994; Dunlap et al., 1995). ω-CTx-GVIA is thought to bind to the outer mouth of the N-type Ca^{2+} channel (McCleskey et al., 1987; Ellinor et al., 1994). Because the three-dimensional structures of ω-CTx-GVIA and other ω-conotoxins are known from nuclear magnetic resonance (Pallaghy et al., 1993; Sevilla et al., 1993; Basus et al., 1995; Farr-Jones et al., 1995; Nemoto et al., 1995), analysis of the toxin-channel interaction might provide valuable information about the outer vestibule of the Ca^{2+} channel.

As structural probes, peptide toxins have the potential of reporting dynamic as well as static aspects of channel structure. Modulation of block by changes in gating is well known for smaller molecules such as quaternary ammonium compounds (Armstrong, 1969, 1971), local anesthetics (Hille, 1977; Hondeghem and Katzung, 1977), organic Ca^{2+} channel blockers (Lee and Tsien, 1983; Bean, 1984), and sulfhydryl-reactive reagents (Yang and Horn, 1995; Larsson et al., 1996; Liu et al., 1996). Peptide toxins offer advantages as probes of voltage-dependent conformational changes because their effects are potent and specific and their site of action is unequivocally extracellular.

Inactivation is an important aspect of Ca^{2+} channel gating, critical for governing the amount of Ca^{2+} entry during repetitive firing (Carbone and Swandulla, 1990; Pelzer et al., 1990). Although the kinetics of voltage-dependent inactivation differs strikingly among Ca^{2+} channel types, it is not clear whether Ca^{2+} channel inactivation involves internal or external conformational changes or both. One possible internal mechanism is the rapid occlusion of the open channel by a tethered intracellular blocking group, as proposed for the N-terminal domain of K^+ channels (Zagotta et al., 1990) or the intracellular III–IV loop in Na^+ channels (Vassilev et al., 1988; Stühmer et al., 1989; Catterall, 1993). Another possible mechanism is a conformational change near the external mouth of the Ca^{2+} channel pore, analogous to C-type inactivation of K^+ channels, which affects K^+ channel interactions with extracellular Cd^{2+}, tetraethylammonium$^+$, and sulfhydryl modifiers (Hoshi et al., 1990; Choi et al., 1991; López-Barneo et al., 1993; Yellen et al., 1994; Baukrowitz and Yellen, 1995; Liu et al., 1996). Questions about possible external conformational changes in Ca^{2+} channels are of further interest because subtype-specific differences in voltage-dependent inactivation kinetics have been traced to residues in membrane-spanning segment IS6 and nearby extracellular and cytoplasmic regions (Zhang et al., 1994). Here we explore such issues by examining the effects of a series of ω-conotoxins, focusing on the question of whether their potency is dependent on the gating state of the N-type Ca^{2+} channel.

Received Nov. 28, 1996; revised Feb. 18, 1997; accepted Feb. 20, 1997.

This research was supported by grants from National Institutes of Health (R.W.T., R.W.A.) and a training grant in cardiac electrophysiology (National Institutes of Health) (J.W.S.). R.W.A. is an investigator of the Howard Hughes Medical Institute. We are grateful to P. T. Ellinor, W. A. Horne, and T. Tanabe, V. Flockerzi, and F. Hofmann for cDNAs for α_{1B} subunits, α_2/δ subunits, and β_1 subunits, respectively. We thank Ilya Bezprozvanny and Xiao-Hua Chen for helpful discussions and Rebecca Agin for skilled technical support.

Correspondence should be addressed to Dr. Richard W. Tsien, Department of Molecular and Cellular Physiology, Beckman Center, B105A, Stanford, CA 94305-5426.

Dr. Stocker's present address: ICAgen, Inc., 4222 Emperor Boulevard, Durham, NC 27703.

MATERIALS AND METHODS

Preparation of Xenopus *oocytes and expression of channels.* Ovarian tissue was removed from anesthetized female *Xenopus laevis*. Stage V–VI oocytes free of follicular cells were obtained after incubation with shaking for 2 hr in a Ca^{2+}-free solution (82.5 mM NaCl, 2 mM KCl, 1 mM $MgCl_2$, and 5 mM HEPES, pH 7.5) containing 1 mg/ml collagenase A as described previously (Sather et al., 1993). The oocytes were washed and transferred to a storage medium (96 mM NaCl, 2 mM KCl, 1.8 mM $CaCl_2$, 1 mM $MgCl_2$, and 5 mM HEPES, pH 7.6, with 2.5 mM sodium pyruvate and the antibiotics gentamycin, penicillin, and streptomycin).

Selected oocytes were then stored at 18°C for several hours or overnight before injection. Expression of calcium channels was achieved by injection of α_{1b} with α_2/δ and β_{1a} cRNA that had been dissolved in water and mixed in approximately equimolar ratios. The cRNAs were synthesized *in vitro* using T7 or SP6 polymerase from corresponding cDNAs, an α_{1b} construct largely derived from human hippocampal cDNA (Ellinor et al., 1994), α_2/δ (courtesy of Prof. T. Tanabe) and β_{1a} (Ruth et al., 1989). Details about the composition of these subunits are given in the earlier papers cited.

Electrophysiological recordings and toxin application. Whole-cell Ba^{2+} currents were recorded using a two-electrode voltage-clamp amplifier (model OC-725A, Warner Instruments, Hamden, CT). Current-passing and voltage-measuring electrodes were filled with 3 M KCl and typically had resistances in the range of 1–5 MΩ. The potential of the bath was measured by a chlorided silver wire immersed in a reservoir filled with 3 M KCl connected to the chamber by a 3 M KCl–agar bridge. A chlorided silver wire placed directly in the recording chamber was used to measure the amount of current injected by the current electrode.

Ba^{2+} current through the expressed Ca^{2+} channels was induced by stepping the holding potential (HP) to 0 mV for test pulse with a 50 msec duration. Intrapulse duration was varied between 5 sec and 1 min depending on the total time of a given experimental run and the time resolution desired. The current signal was filtered at 500 Hz (Frequency Devices, Haverhill, MA) and processed using Axon Basic-based programs (Axon Instruments, Foster City, CA). Leak traces were taken using a −P/4 protocol and subtracted off-line.

For current measurements, oocytes were placed in a perfusion solution containing 5 mM $Ba(OH)_2$, 2 mM KOH, 85 mM tetraethylammonium, and 5 mM HEPES, with pH adjusted to 7.4 with methanesulfonic acid. In addition, all of the solutions contained 0.1 mg/ml cytochrome c to saturate nonspecific binding sites. During recording, the oocytes were perfused continuously at a rate of ~0.5 ml/min. The ω-conotoxins GVIA (Peninsula Laboratories), MVIIA (The Peptide Institute), MVIIC (SNX-230), TVIA (SNX-185), and SNX-331 (Neurex) were all initially dissolved in water at the stock concentration of 1.0 mM and stored at −20°C. Fresh dilutions of the peptides into the 5 mM Ba^{2+} perfusion solution were made immediately before use. Application of ω-conotoxins was achieved by complete perfusion of the recording chamber with solution containing a given peptide.

RESULTS

Voltage-dependent block of N-type calcium channels by an ω-conotoxin

During the course of characterizing a series of ω-conotoxins, we found evidence that their ability to block N-type Ca^{2+} channels is strongly voltage-dependent. This was seen most dramatically with SNX-331, the Y13W derivative of the well known ω-conotoxin ω-CTx-MVIIC (Fig. 1*A*). The rapid onset and recovery from block seen after application and washoff of SNX-331 made it advantageous for use in this study. The availability of N-type Ca^{2+} channels was assessed by monitoring the peak current elicited by a brief test pulse to 0 mV. The kinetics of the development and removal of block was strongly affected by the membrane potential at which the oocyte was maintained (HP). At a strongly hyperpolarized potential (*HP* = −120 mV), both the onset and recovery from block appeared to follow simple exponential time courses. In contrast, at a less negative potential (*HP* = −70 mV), much more complex behavior was seen. In this case, the onset of block by SNX-331 was strikingly biphasic, consisting of an initial rapid phase, very much like that observed at the strongly negative HP, followed by a much slower phase that required at least 10 min of toxin exposure to approach completion. Likewise, the removal of blockade after washoff of toxin at −70 mV was also complex. A small fraction of current recovered rapidly, with a time course similar to that found at −120 mV, but after completion of this phase, a large portion of the overall current remained inhibited.

The incompleteness of recovery was not caused by rundown or some irreversible effect of the conotoxin, as illustrated by the protocol in Figure 1*B*. After application and removal of SNX-331 (5 μM in this case) at the depolarized potential of −70 mV, a partial rapid recovery of current is observed similar to that in Figure 1*A*. After the initial partial recovery, a change of the *HP* to −120 mV yielded a dramatic and rapid recovery from the remaining block. Relief of the block at the hyperpolarized potential appears complete in that the larger peak current level obtained at an *HP* of −120 mV can be accounted for by the greater availability of channels in the resting (R) state at that potential (Fig. 3*A*). As a further test of the voltage dependence of block, reapplication of SNX-331 yielded a block that could be rapidly and completely removed after toxin washoff in contrast to the long-lived blocking behavior observed at the more depolarized potential in the same oocyte.

Voltage-dependent effects of ω-CTx-GVIA and other conotoxins

This robust voltage-dependent interaction with the N-type calcium channel was not only seen with SNX-331. A variety of toxins, including the commonly used GVIA, MVIIA, TVIA, and MVIIC, were tested for their voltage-dependent interaction with Ca^{2+} channels. Application of each of the toxins at an *HP* of −80 mV gave a rapid block of current (Fig. 2). After washoff, no or very little recovery of current was observed for any of the four toxins (Fig. 2); however, after hyperpolarizing the oocyte to an *HP* of −120 mV, the rate of recovery showed an immediate and dramatic increase. Although still slow, a nearly complete recovery of block was observed for three of the four toxins tested after ~1 hr (Fig. 2). Although the voltage dependence of recovery from block appears most dramatic with SNX-331 because of its intrinsically rapid rate of block and unblock, a wide variety of other ω-conotoxins appear to show some degree of voltage-dependent interaction with N-type Ca^{2+} channels.

Correlation between degree of channel inactivation and changes in toxin-blocking characteristics

The influence of membrane depolarization on the degree of block might be interpreted in a number of ways. One possibility, based on well described actions of local anesthetics on Na^+ channels and Ca^{2+} channel blockers on L-type Ca^{2+} channels, is that the strength of toxin binding depends on the state of the channel, as in the classic modulated receptor hypothesis (Hille, 1977; Hondeghem and Katzung, 1977). In the simplest version of this hypothesis (Fig. 3*A*, *inset*), toxin binds more strongly to channels in the inactivated (I) state than to those in the R state, thus giving rise to a voltage dependence of block. As a test of this idea, we looked for a relationship between the degree of inactivation and the characteristics of the toxin block. The voltage dependence of inactivation was determined using a conventional protocol (Fig. 3*A*). As the *HP* was varied between −120 mV and −30 mV, the peak current during a test depolarization to 0 mV gradually diminished, indicating that an increasing proportion of channels had become inactivated. A slight degree of inactivation was ob-

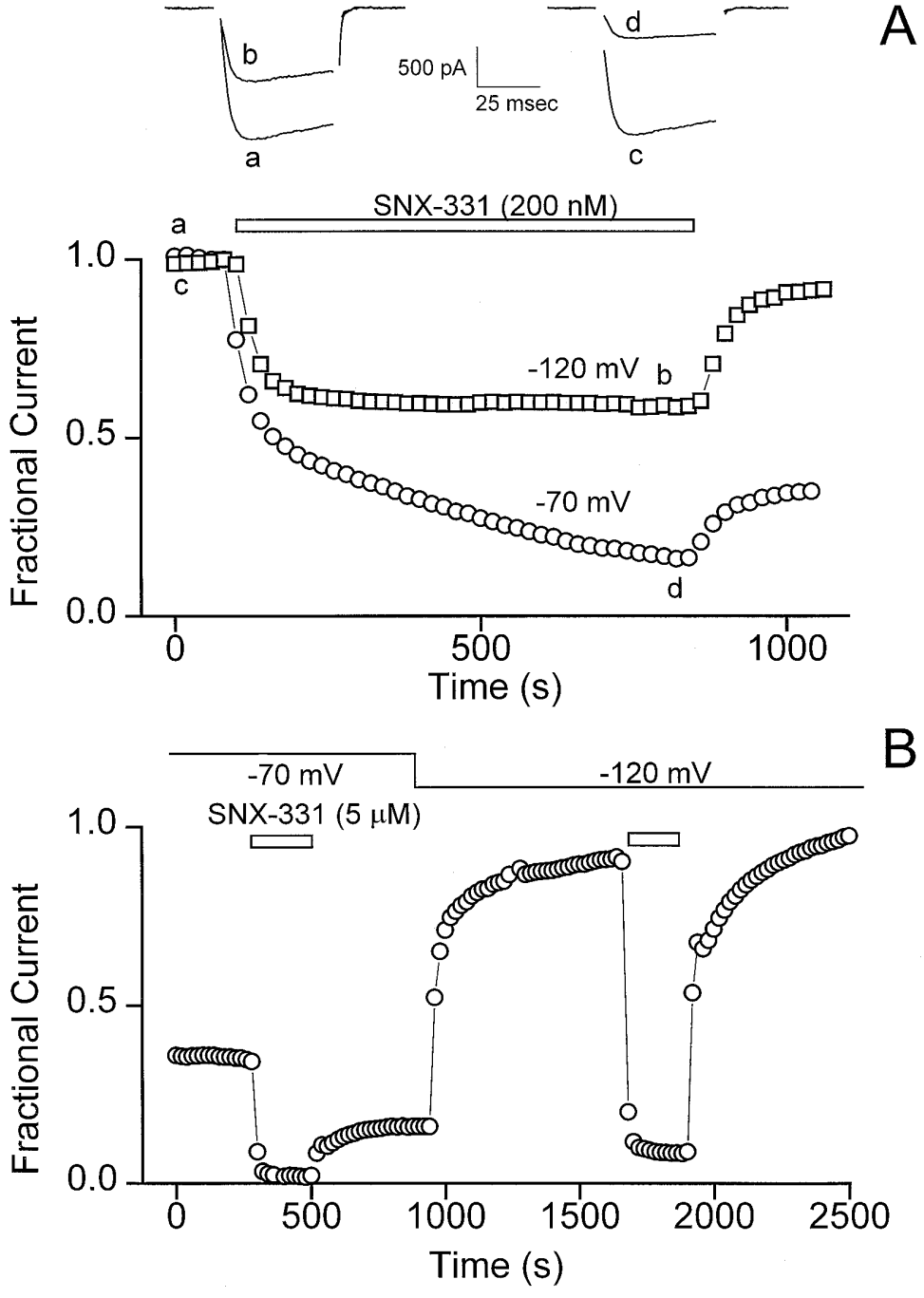

Figure 1. Ca^{2+} channel block by conotoxin is highly voltage-dependent. *A*, The blocking characteristics of SNX-331 (200 nM) applied to N-type Ca^{2+} channels expressed in *Xenopus* oocytes are shown for two different *HPs*: −120 mV and −70 mV. Test currents were evoked by stepping to 0 mV at 20 sec intervals, and peak current values were plotted as a function of time. Sample traces of the test current are shown at the times indicated by *lower case letters*. Results from this exemplar oocyte are representative of more than five experiments. *B*, A partial recovery from block is observed after application and washout of SNX-331 (5 μM) at the *HP* of −70 mV, similar to that seen in *A*, but rapid relief of this block occurs after hyperpolarizing the oocyte to an *HP* of −120 mV. A second application of SNX-331 at the *HP* of −120 mV gives a block, which after washoff of toxin yields rapid and complete recovery of current. Illustrative results from this exemplar oocyte are representative of seven experiments.

served at −90 mV, half inactivation was achieved at approximately −70 mV, and complete inactivation was obtained near −40 mV (Fig. 3*A*), in line with previous work on cloned N-type Ca^{2+} channels (Williams et al., 1992; Fujita et al., 1993; Ellinor et al., 1994; Bezprozvanny and Tsien, 1995).

The modulated receptor hypothesis in its simplest form predicts that the characteristics of toxin block should be governed entirely by the gating properties of the channel. Accordingly, the time course and extent of block should remain unaltered over a voltage range in which the gating state is not changed. We tested this by examining properties of toxin block at potentials at which the occupancy of the R state had reached saturation: −100 mV and −120 mV (Fig. 3*A*). As predicted, the characteristics of onset and removal of toxin block were indistinguishable at these levels of HP (Fig. 3*B*). In contrast, at an *HP* of −70 mV, in which ~50% of the channels are in the I state, a dramatic difference was observed in both the blocking and unblocking characteristics. The same concentration of SNX-331 caused a significantly greater degree of inhibition, and the block displayed a biphasic onset and only partial recovery. Thus, changes in the balance between the R and I states are correlated with differences in toxin block.

The absence of a significant difference between the blocking behavior at −100 mV and −120 mV runs counter to a scenario in which the membrane electric field exerts a direct effect on the local concentration of toxin near its receptor site. This interpretation seems unlikely in any case, because, if anything, depolarizations should decrease the local concentration of the positively charged ω-conotoxin, thereby diminishing its blocking effect.

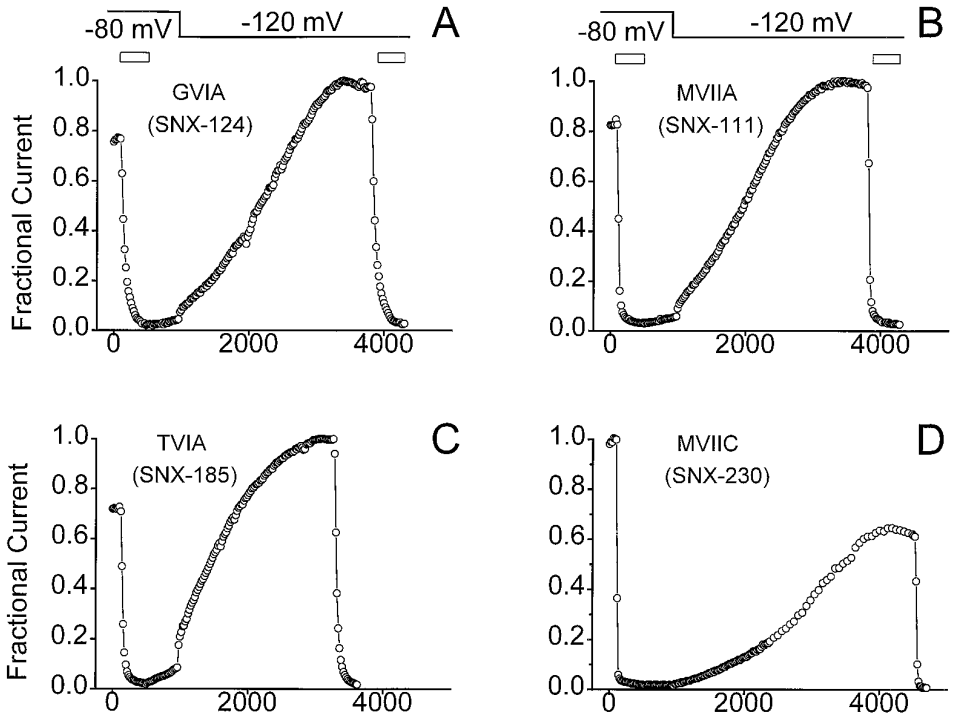

Figure 2. Voltage-dependent relief of block seen for GVIA, MVIIA, TVIA, and MVIIC. GVIA (*A*), MVIIA (*B*), TVIA (*C*), and MVIIC (*D*) (all at 5 μM) were applied to oocytes expressing the N-type Ca^{2+} channels initially held at −80 mV. After 7 min of toxin application, washout at the same HP gave very little recovery of current. After an initial 7 min of washout at −80 mV, the *HP* of the oocyte was stepped to −120 mV, which evoked a more rapid rate of current recovery. After what appeared to be complete recovery of current, a second application of toxin was given to ensure that this recovered current was still sensitive to block. Results illustrate behavior observed in multiple oocytes ($n = 3$ for each toxin).

Affinity of SNX-331 for the R state of the channel

As a further test of the modulated receptor scheme, we set out to characterize the interaction of the toxin with R and I states of the channel and to determine to what extent these were different. Determination of the affinity of the toxin for the R state was relatively straightforward. As a standard procedure, the membrane potential was held at −120 mV, at which the vast majority of the channels are in the R state, and the blocking effect of SNX-331 was monitored over a wide range of concentrations (Fig. 4). After application of the toxin, the amplitude of the peak current decreased with an exponential time course toward a lower, steady level (Fig. 4*A*). The percentage of current remaining at various toxin concentrations conformed reasonably well to a dose–response relationship describing one-to-one block (Fig. 4*B*). Half-block was attained at 180 nM toxin, giving an approximate estimate of the dissociation constant to the R state (K_R). The approach to steady state was relatively quick at the negative HP. The rate constants (τ^{-1}) for toxin block showed a linear dependence on toxin concentration, as expected for a first-order reaction (Fig. 4*C*). The slope of this dependence provided an estimate of the on-rate for toxin block (k_{on}), 4×10^4 $M^{-1} \cdot sec^{-1}$, and the *y*-intercept gives an off-rate (k_{off}) of 2.8×10^{-2} sec.

Affinity of SNX-331 for the I state of the channel

Determination of the toxin's affinity for the I state of the channel cannot be made as directly because complete inactivation of the channels leaves no current to be measured. However, it is possible to characterize the toxin's affinity for channels under less extreme conditions and extract an estimate of the dissociation constant for the I state (K_I). According to the modulated receptor hypothesis, the apparent affinity of toxin at any given HP should be the weighted sum of the affinities for the various states (Bean et al., 1983). Considering only R and I states for the moment,

$$K_{app}^{-1}(V) = h_\infty(V) \cdot K_R^{-1} + \{(1 - h_\infty(V)) \cdot K_I^{-1}\} \quad (1)$$

where $K_{app}(V)$ is the K_D of toxin for channel, and $h_\infty(V)$ is the fraction of available channels. Because K_R and $h_\infty(V)$ were determined previously, a measurement of K_{app} is sufficient to determine K_I. We chose to do this with an *HP* of −70 mV, where $h_\infty(V) \cong 0.5$.

The potency of the toxin was clearly greater at −70 mV than at −120 mV (Fig. 5*A*). For example, 1 nM SNX-331 reduced the peak current by at least one-third at the depolarized potential, whereas it had no detectable effect at the more hyperpolarized potential (Fig. 4*A*). Likewise, inhibition by 10 nM toxin was >60% at −70 mV and <10% at −120 mV. Figure 5*B* shows the dose dependence of the fractional current remaining 20 min after beginning the application of SNX-331. This duration of toxin exposure allowed block to come reasonably close to steady state even at the lowest toxin concentrations but avoided the rundown seen in control experiments over much longer periods. The percentage of block at various conotoxin concentrations was roughly fit with a theoretical binding curve, yielding a value of $K_{app}(-70)$ of 6 nM. Using Equation 1 and taking $h_\infty = 0.5$ and $K_R = 180$ nM, the calculated value of K_I is ~3 nM. This represents an ~60-fold increase in affinity relative to the R state. The estimated change in affinity must be regarded as a lower limit, because the toxin-channel interaction may fall short of equilibrium even after 20 min.

Varying residency in the open state has no detectable effect on toxin block

Having found a large difference between R and I states with respect to the apparent affinity of SNX-331, we went on to consider the possibility of preferential interactions with the channel's open state. A series of experiments was conducted to see whether toxin blocking characteristics might be altered as a result of modifying the proportion of time the channels spent in the open state (Fig. 6). Test-pulse durations of 25, 50, or 250 msec were used during application of SNX-331 (1 μM), with the cycle

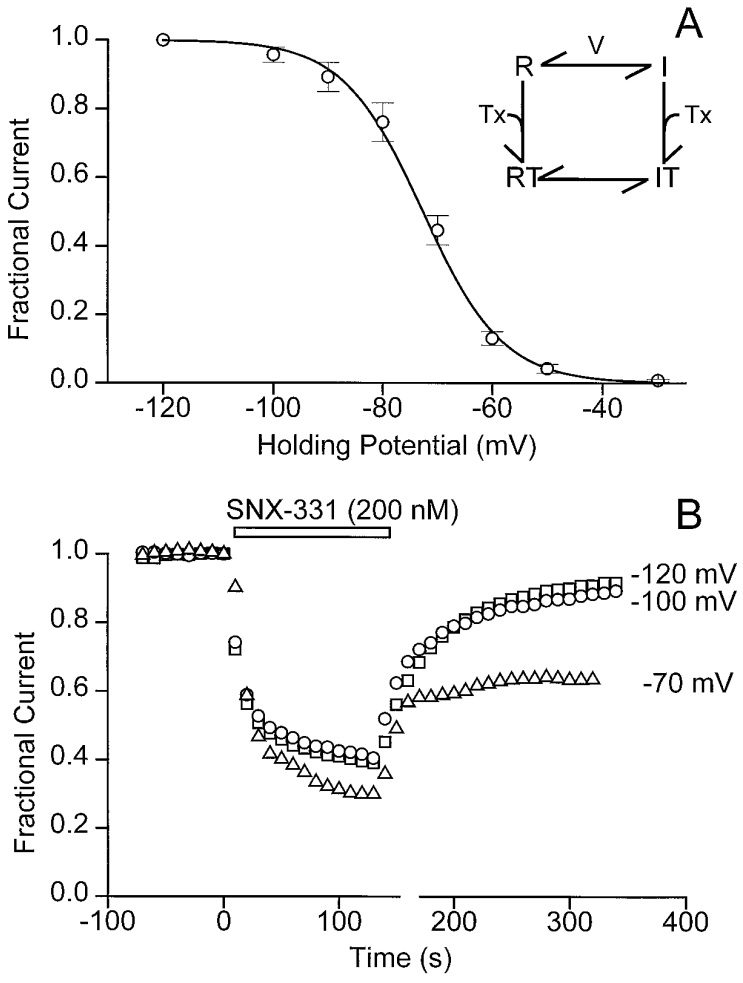

Figure 3. Correlation between channel inactivation and blocking characteristics of conotoxin. *A*, A steady-state inactivation curve for the N-type Ca^{2+} channels expressed in *Xenopus* oocytes was generated by measuring channel availability as a function of HP. The holding voltage was stepped from −120 mV to −30 mV, and channels were held at each HP for 5 min before giving the test pulse. The peak current at $HP = -120$ mV was normalized to 1 (i.e., 100% of the channels are estimated to be in the R state), and the data were fit by a Boltzmann relationship: $I(V) = 1/(1 + \exp((V - V_{1/2})/k))$, where $V_{1/2} = -72.7$ mV and $k = 7.3$ mV. The results shown are the average of five trials ± SD. *B*, The blocking characteristics of SNX-331 (200 nM) were monitored at three different HPs. With test currents being evoked every 10 sec, characteristic onset of and recovery from block after application and washoff of SNX-331, respectively, was observed for three different oocytes being held at the *HPs* of −120, −100, and −70 mV.

time fixed at 5 sec. Because inactivation was incomplete even after a 250 msec depolarization, this procedure resulted in a large variation in the fraction of time spent in the open state (Fig. 6, *inset*). There was no appreciable difference in the time course of onset of block or the steady-state degree of block as the test-pulse duration was lengthened 10-fold. Likewise, these properties remained unchanged when the frequency of pulses was varied between once every 30 sec and once every 5 sec (data not shown). The process of channel inactivation put practical restrictions on the percentage of the overall duty cycle that could be spent at the test potential level. Within these limitations, it is clear that differences in toxin affinity for R and open states of the channel could not be detected under the present experimental conditions.

Simulation of voltage-dependent block by a modulated receptor scheme

A critical test of the applicability of the modulated receptor hypothesis is to determine whether it can simulate the kinetics of the toxin-channel interaction in a realistic manner (Fig. 7). We attempted this using the simplest modulated receptor scheme containing only two gating states, R and I, and the corresponding toxin-bound states, RT and IT. Our objective was to see whether this minimal model could predict the major characteristics of block and unblock of ω-conotoxins at both hyperpolarized ($HP = -120$ mV) and depolarized ($HP = -70$ mV) potentials. Inasmuch as possible, the kinetic parameters of the scheme were determined experimentally. k_{on} and k_{off}, the rate constants for toxin binding to and dissociation from the the R state, were based on data obtained at $HP = -120$ mV (Fig. 4). k_{on} was extracted from the slope of the relationship between τ^{-1} and toxin concentration; k_{off} was estimated as $k_{on} \cdot K_R$, where K_R was obtained from the observed dose dependence (Fig. 4*B*). The equilibrium between R and I states was described conventionally by the voltage-dependent rate constants β_h and α_h for development of and recovery from inactivation, respectively. β_h and α_h were constrained to be equal at $HP = -70$ mV, where $h_\infty = \alpha_h/(\alpha_h + \beta_h) = 0.5$ (Fig. 3*A*). At this *HP*, the rate of equilibration between R and I states in *Xenopus* oocytes was found to be exceedingly slow ($\tau \sim 100$ sec) [J. W. Stocker and R. W. Tsien, unpublished data; also seen in native channels in dissociated neurons (Jones and Marks, 1989)], and the values of β_h and α_h were adjusted accordingly. At $HP = -120$ mV, α_h was set at a value 1000-fold greater than β_h to describe an equilibrium greatly in favor of the R state.

The higher affinity of toxin for the I state was embodied in the parameters k'_{on} and k'_{off}, which were adjusted to allow simulations of onset of block to approximate the experimental data at −70 mV (Fig. 5*A*). For toxin-bound forms of the channel, the rate constants for inactivation and recovery from inactivation were β'_h and α'_h. By the principle of microscopic reversibility, the ability of the gating state to affect the toxin interaction must be accompanied by a corresponding influence of bound toxin on the gating

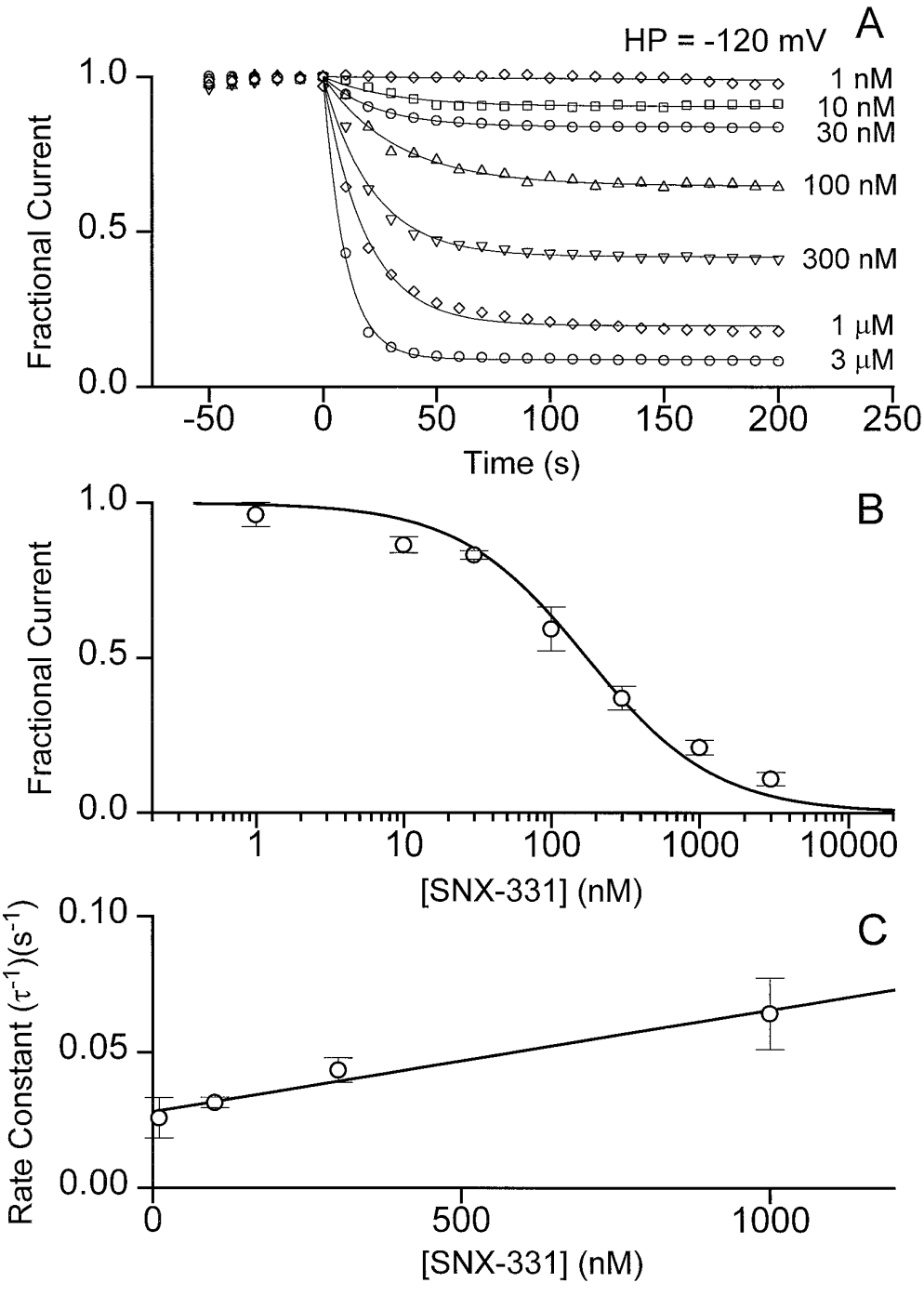

Figure 4. Simple and rapid blockade of current by SNX-331 at an *HP* of −120 mV. *A*, Onset and degree of block by a variety of SNX-331 concentrations covering a 3000-fold range was measured for oocytes held at *HP* = −120 mV. Onset of block at each concentration could be fit well by a single-exponential time course. The steady-state degree of block was determined from the fit to a single-exponential plus a constant. *B*, The amount of current after steady-state block had been reached was determined as in *A*, averaged (n = 5, ±SD), and plotted as a function of toxin concentration. A good fit to the data was achieved using the functional form for a one-to-one binding relationship: $(1/(1 + ([Tx]/K_D)))$, where K_D = 180 nM. *C*, Rate constants for the exponential time course of the onset of block at different toxin concentrations were determined from the data in *A*. The averaged rate constants at four of the intermediate toxin concentrations were plotted as a function of concentration (n = 5, ±SD) and were fit well by the relationship $(\tau)^{-1} = k_{on}[Tx] + k_{off}$, where $k_{on} = 4.0 \times 10^4\ M^{-1} \cdot sec^{-1}$, and $k_{off} = 2.8 \times 10^{-2} \cdot sec^{-1}$.

transition. Accordingly, the scaling that was used to modify the I ↔ IT transition was also applied to the IT ↔ RT reaction, and the steepness of the voltage dependence of $h'_\infty \equiv \alpha'_h/(\alpha'_h + \beta'_h)$ was kept the same as that of h_∞ (Fig. 7, legend). We found that it was necessary at depolarized potentials to set β'_h and α'_h to values considerably slower than β_h and α_h to account for the dynamic and steady-state characteristics of the toxin block.

With parameters assigned in this way, the minimal modulated receptor scheme generates kinetics of channel block and unblock (Fig. 7*B*) that agree reasonably well with the experimental observations at both HPs (Fig. 7*A*). The simple behavior at −120 mV results from toxin association and dissociation from the R state only. The more complex kinetics at *HP* = −70 mV can be understood in terms of the changing occupancy of the four states (Fig. 7*D*). Both resting and inactivated toxin-bound states (RT and IT) undergo an initial rapid increase in occupancy after toxin application at the expense of R and I, accounting for the early rapid decrease in current observed experimentally. During sustained exposure to toxin, channels accumulate in the IT state, causing a continual depletion of channels from all other states, including the R state (Fig. 7*D*), thereby causing the slow second phase of toxin block observed experimentally (Fig. 7*A*). After removal of toxin, recovery from the IT state occurs only very slowly because the dissociation of the toxin (off-rate, k'_{off}) and the rate of recovery from inactivation (α'_h) are both quite slow. A small component of rapid recovery is observed, corresponding to

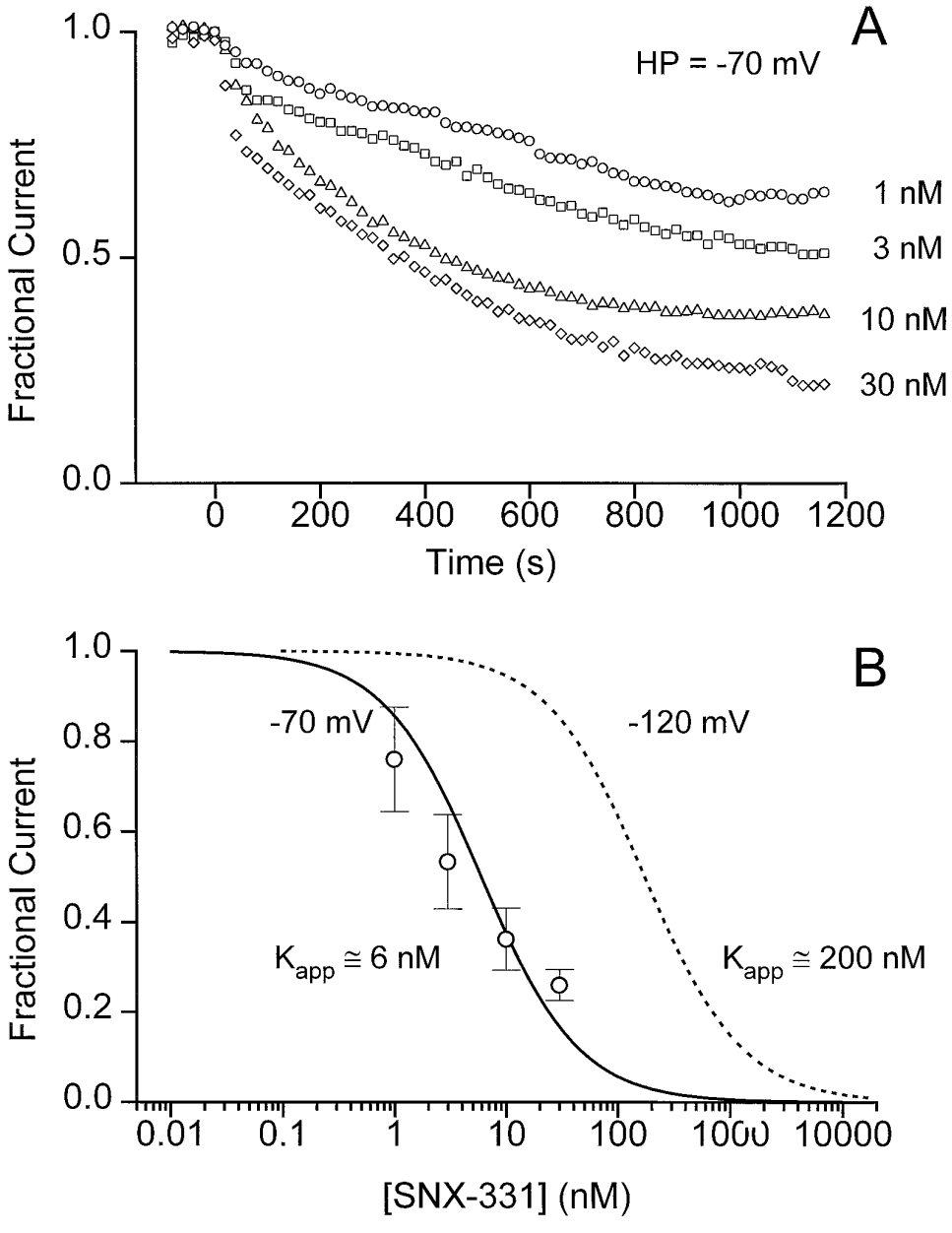

Figure 5. Increase in potency of blockade of current observed at depolarized potentials. *A*, Blockade of current at an *HP* of −70 mV was monitored by applying a variety of SNX-331 concentrations for 20 min. Whereas the onset of block at −70 mV occurred with a much slower time course than that observed at an *HP* = −120 mV, the degree of block at low dosages was also much greater than that observed at −120 mV, indicating a dramatic increase in the efficacy of block at the depolarized potential. *B*, Averaged values of the percentage of current remaining after a 20 min application of SNX-331 were plotted as a function of toxin concentration (n = 4, ±SD). The data were fit to the functional form $(1/(1 + ([Tx]/K_D)))$ to place an upper limit on the estimate of the apparent affinity of SNX-331 for the channel at an *HP* of −70 mV.

the small proportion of channels in the RT state that can quickly make a direct transition to the R state.

Buildup and recovery of slowly recovering fraction are both strongly voltage-dependent

Until now, we have focused on experiments in which the same level of HP was maintained during toxin exposure and washout. These protocols leave open questions about whether the trapping of channels in a long-lasting nonconducting form depends on the gating state of the channels during toxin association, toxin dissociation, or both. To distinguish between these possibilities, we turned to more complex protocols in which toxin was applied at one level of HP and removed at a sharply different HP. Figure 8*A* illustrated an experiment in which the HP was switched between −80 mV and −120 mV in various possible combinations in the presence and absence of applied SNX-331. When toxin application was carried out at the relatively depolarized potential but removed at the strongly negative potential (trial 1), a rapid and complete recovery of current ensued (compare with recovery after trial 4). Likewise, when toxin was applied at a hyperpolarized potential followed by washoff at a depolarized potential (trial 2), the current after washoff returned to its pretoxin, depolarized HP level (i.e., before trial 1) without indication of trapping. These results are in sharp contrast to the prominent trapping observed when toxin application and washoff were both performed at *HP* = −80 mV (trial 3).

These experiments provided an additional opportunity for testing the validity of the modulated receptor hypothesis with regard to conotoxin block. As shown in Figure 8*B*, the minimal model correctly simulates all the essential features of the experimental results. In the context of the model, strong hyperpolarization is able to alleviate trapping of channels in the IT state because it greatly speeds the recovery from IT→RT→R. On the other hand, the application of toxin at a hyperpolarized potential allows only

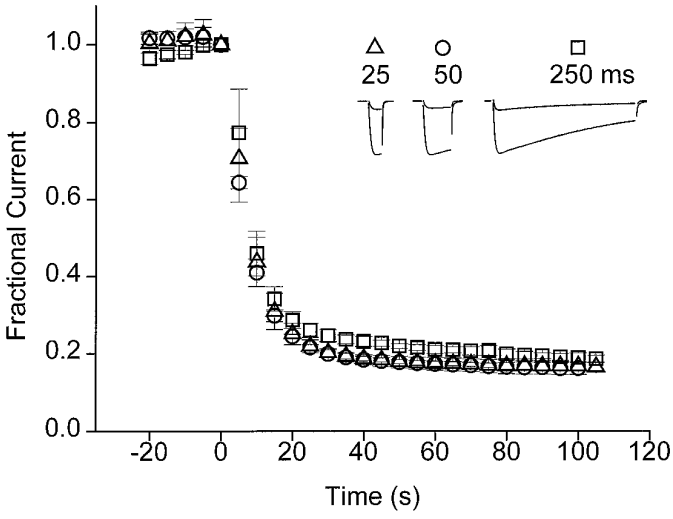

Figure 6. Variation of the total amount of time spent in the open state has no effect on toxin block. Blockade of current after application of SNX-331 (1 μM) was monitored while varying test-pulse duration. The *HP* during the duration of the experiment was −120 mV, and all test pulses were to 0 mV. The cycle time between pulses was kept at a constant 5 sec, and the duration of pulses was varied between 25, 50, and 250 msec. Each point represents the average of data from four experiments.

a very small population of channels to ever reach the IT state, so that little trapping is found even if the washout is performed at the relatively depolarized potential.

DISCUSSION

The discovery of a marked potential dependence of ω-conotoxin block of N-type Ca^{2+} channels, not anticipated from earlier studies, has important implications. As we discuss below, it reflects the ability of the ω-conotoxin to discriminate between resting and inactivated states of the channel, a feature not previously reported for a peptide toxin and a Ca^{2+} channel. The enhancement of toxin affinity after steady depolarization bears relevance to biochemical and cell biological experiments in which ω-conotoxins serve as labels of N-type Ca^{2+} channels, and to physiological studies in which the toxin is used to dissect their contributions. Finding that a peptide toxin can interact preferentially with a voltage-gated Ca^{2+} channel after its inactivation provides a fresh perspective on the structural changes that accompany this form of gating.

Importance of voltage-dependent interaction for studies using ω-conotoxins

Membrane depolarization strongly affected the interaction between N-type Ca^{2+} channels and ω-conotoxins. Although this was observed most clearly in the case of SNX-331 because of its relatively rapid rate of dissociation, a marked voltage dependence was a general finding for other members of the ω-conotoxin family, including ω-CTx-GVIA, ω-CTx-MVIIA, ω-CTx-MVIIC and ω-CTx-TVIA (Fig. 2). In all cases, membrane hyperpolarization to strongly negative HPs sharply accelerated the removal of block after washout of ω-conotoxin, allowing a complete recovery. This is a striking result, because the blocking effects of toxins such as ω-CTx-GVIA have been considered largely or completely irreversible on the time scale of electrophysiological experiments. Variations in voltage protocol may have contributed to the partial recovery in those few cases in which it has been reported (Aosaki and Kasai, 1989; Plummer et al., 1989; Ellinor et al., 1994).

Our results open up new possibilities for experiments using ω-conotoxins such as ω-CTx-GVIA. The ability to remove ω-conotoxin inhibition at strongly hyperpolarized potentials could be very useful in experiments in which reversibility of blockade of N-type channels is important. An equilibration between toxin and channel can be characterized on the time scale of electrophysiological recordings, making quantitative studies of structural relationships between mutant channels and variant toxins possible (cf. Hidalgo and MacKinnon, 1995). However, our experiments also reveal the need for caution in the interpretation of experiments that rely on ω-conotoxins to define properties of N-type channels or their physiological contributions. Special care must be taken when comparing experimental results acquired under conditions in which membrane potential varies or is undetermined. For example, toxin block in cells with negative resting potentials will show properties very different from characteristics of toxin binding to depolarized membrane fragments, thus explaining previous discrepancies between radioligand binding (picomolar dissociation constants) and electrophysiology (nanomolar IC_{50}s) (for an analogous case, see Bean, 1984).

Interpretation of the voltage dependence of blockade

The mechanism of the potential-dependence of ω-conotoxin block was of considerable interest. It cannot be explained by a movement of the toxin's positive charge along the membrane electric field, in which case hyperpolarization would promote blockade. The relief of ω-conotoxin inhibition by hyperpolarization that was observed contrasts with the voltage dependence of α-scorpion toxin binding to neuronal Na^+ channels, which greatly increases in affinity the more negative the membrane potential (Catterall, 1977), and that of tetrodotoxin and saxitoxin block of skeletal muscle Na^+ channels, which is accentuated at negative potentials in proportion to toxin charge (Satin et al., 1994).

Another scenario for voltage dependence is an electrostatic interaction between the cationic toxin and the positive charges of the voltage-sensing machinery. However, the predicted effect would be a relief of block with increasing depolarization, once again in conflict with the observed voltage dependence. Thus, blockade of N-type channels by ω-conotoxins differs from blockade of P-type Ca^{2+} channels by ω-Aga-IVA, which is relieved by very strong depolarizations, presumably reflecting antagonism between toxin binding and activation (Mintz et al., 1992; Randall and Tsien, 1995). Similarly, in Na^+ channels, a partially blocking form of μ-conotoxin can oppose voltage-dependent activation (French et al., 1996).

Our experiments demonstrated that the characteristics of toxin block changed in accordance with the degree of inactivation. The potency of block was greatly enhanced at depolarized HP levels that promote inactivation (Fig. 5); at the other extreme, over a voltage range in which inactivation was completely removed, the characteristics of block showed no detectable voltage dependence (Fig. 3). These observations led to the proposal that the conotoxin has greater affinity for inactivated channels than for those at rest.

Numerical simulations were carried out to see whether the voltage and time dependence of ω-conotoxin block could be accounted for by a classical modulated receptor scheme (Figs. 7, 8). We focused mainly on a four-state kinetic scheme comprised of the normal R and I states and their toxin-bound counterparts

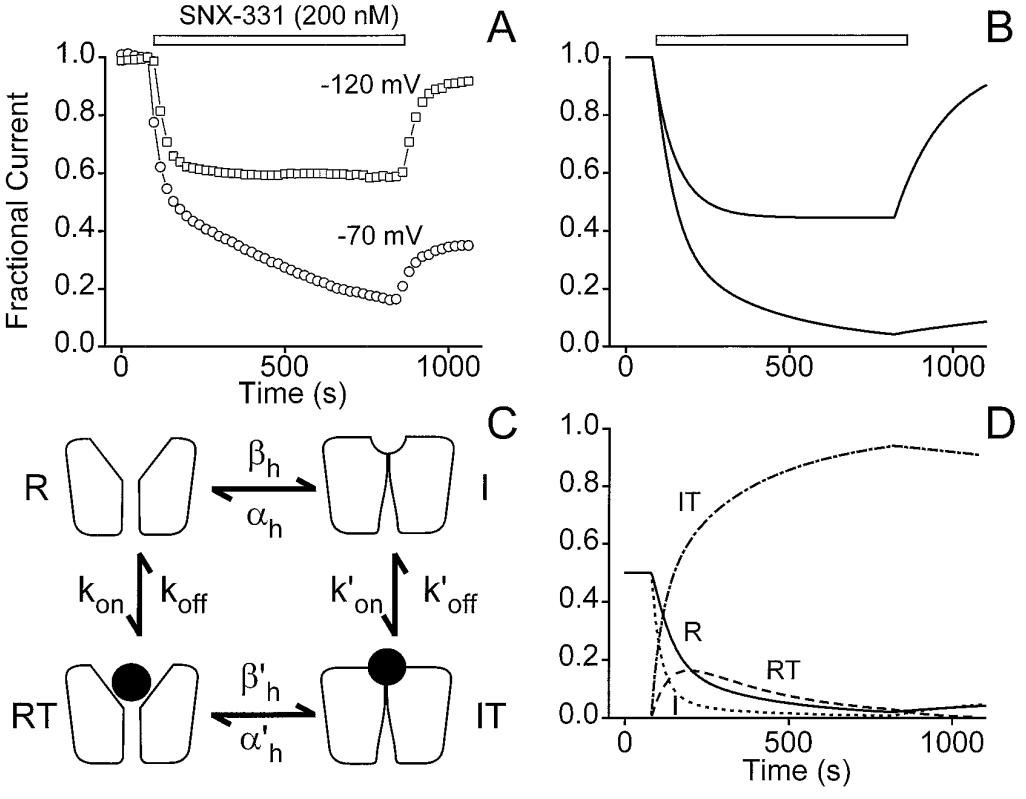

Figure 7. Simulation of voltage-dependent block by a modulated receptor scheme. An attempt to model the voltage dependence of block (*A*) using the modulated receptor scheme diagrammed in *C* yielded the results shown in *B*. The data in *A* showing the voltage dependence of toxin-blocking characteristics are identical to that shown in Figure 1*A*. Good agreement is observed between a comparison of data (*A*) with the predictions made by the model (*B*). The modulated receptor scheme used to generate the predicted blocking behavior includes four states of the channel; resting (*R*), inactivated (*I*), resting with toxin bound (*RT*), and inactivated with toxin bound (*IT*). Appropriate differential equations were solved numerically with Matlab (fourth and fifth order Runge–Kutta formulas for integration). The parameters shown in *C* were given the following values: $k_{on} = 4 \times 10^4$ $M^{-1} \cdot sec^{-1}$, $k_{off} = 8 \times 10^{-3}$ sec^{-1}, $k'_{on} = 1.6 \times 10^5$ $M^{-1} \cdot sec^{-1}$, $k'_{off} = 1.368 \times 10^{-4}$ sec^{-1}, $\beta_h(-70\ mV) = \alpha_h(-70\ mV) = 0.01$ sec^{-1}, $\beta_h(-120\ mV) = 2 \times 10^{-4}$ sec^{-1}, $\alpha_h(-120\ mV) = 0.2$ sec^{-1}, $\beta'_h(-70\ mV) = 4 \times 10^{-4}$ sec^{-1}, $\alpha'_h(-70\ mV) = 1.71 \times 10^{-6}$ sec^{-1}, $\beta'_h(-120\ mV) = 8 \times 10^{-3}$ sec^{-1}, and $\alpha'_h(-120\ mV) = 3.42 \times 10^{-2}$ sec^{-1}. The fractional populations of the four states of the model are plotted separately in *D* for the case in which toxin is applied and washed out at the depolarized potential of −70 mV. The rapid buildup of a large population of channels in the inactivated toxin-bound state (*IT*) during application of toxin can be easily seen.

(RT and IT). The omission of an open state was justified by the observed lack of dependence of blockade on residency in the open state under our experimental conditions (Fig. 6). The treatment of inactivation as a one-step R ↔ I reaction is undoubtedly a simplification, given repeated observations of multiexponential time courses for both channel inactivation and recovery from inactivation (Bezprozvanny et al., 1995; see below). The four-state scheme is merely a minimal model, with the advantage of simplicity.

The rate constants interconnecting the four states were based as closely as possible on direct experimental observations. Data on the voltage and time dependence of inactivation were used to model the equilibrium between R and I states; the observed kinetics of toxin block at −120 mV, at which inactivation was negligible, was used to describe the R ↔ RT transition. Data obtained at −70 mV provided constraints on properties of the I ↔ IT transition. Parameters were given values that maintained the microscopic reversibility of the overall system at any given potential. Within the bounds of these extensive constraints, the minimal four-state model was able to simulate the essential features of block and unblock by SNX-331 at both strongly negative and depolarized HPs (Fig. 7) and at various toxin concentrations (simulations not shown). In particular, the scheme was successful in accounting for the observed kinetic behavior at depolarized potentials—the biphasic onset of block and the partial recovery from block after removal of toxin. Both characteristics were explained by the trapping of channels in the inactivated, toxin-bound (IT) state (Fig. 7*D*). In the simulations, trapping is relieved at strongly hyperpolarized potentials because of the steep voltage dependence of α'_h. The overall conclusion of the modeling is that the voltage dependence of block can be satisfactorily explained by preferential binding to the I state, within the framework of the modulated receptor hypothesis.

Implications for the mechanism of voltage-dependent inactivation

Peptide toxins have been widely used as probes of channel structure, most extensively in studies of the outer vestibule of K^+ channels (Stampe et al., 1994; Aiyar et al., 1995; Ranganathan et al., 1996). It is particularly interesting to find a clear case in which a peptide toxin interacts preferentially with a voltage-gated channel in its inactivated state (cf. Liu et al., 1996). The ω-conotoxins are large, highly charged molecules effective as blockers when applied outside cells (McCleskey et al., 1987), but not when delivered inside (Feldman et al., 1987). Because toxin blockade can occur only through interaction with an extracellular aspect of the channel, a preferential interac-

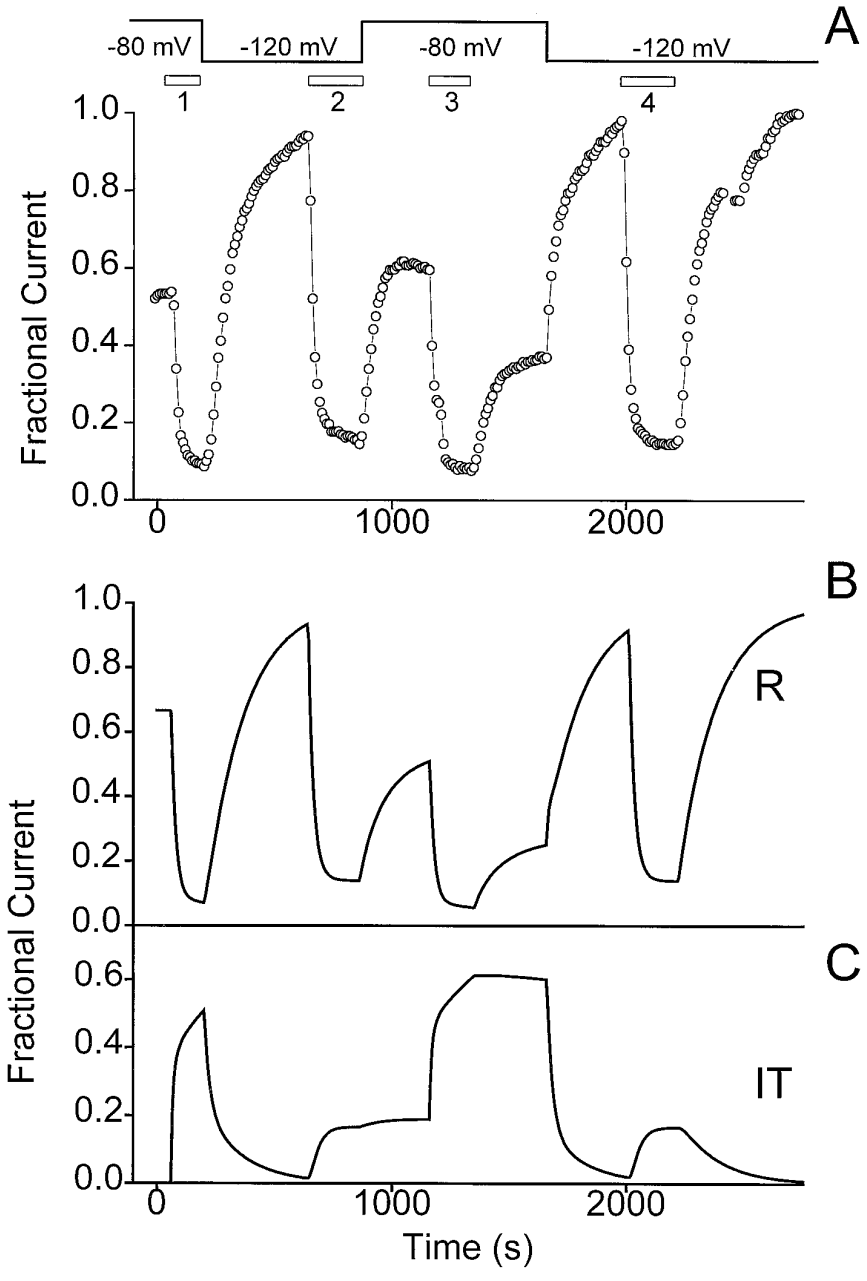

Figure 8. Both buildup and relief of block from the slowly recovering fraction of channels are strongly voltage-dependent. *A*, A protocol was used to investigate the blocking characteristics of toxin when application and washout occur at different HPs. First, SNX-331 (1 μM) was applied at an *HP* = −80 mV. Washoff of toxin occurred with a concomitant change in the *HP* to −120 mV. After recovery of current, SNX-331 was applied again, but now with the oocyte held at −120 mV, and washoff after this application occurred at an *HP* of −80 mV. In the last two segments of this protocol, the same HP is maintained throughout toxin application and washoff. Toxin application and washoff is first done at an *HP* of −80 mV. Full recovery of current is then achieved by hyperpolarizing the cell to −120 mV, and application and washoff of toxin at this hyperpolarized potential follows. *B*, Using the same modulated receptor scheme and parameters as in Figure 7, a model of the expected peak current levels during the above given protocol was generated. *C*, Plot of the fractional population of the I state of the channel with toxin-bound (*IT*) as predicted by the modulated receptor scheme.

tion with the inactivated channel must mean that inactivation is accompanied by an externally detectable conformational change. The locus of this structural change can be narrowed further if ω-conotoxin binds near the mouth of the pore, as suggested by several lines of evidence. All four motifs of the N-type Ca^{2+} channel contribute to its interaction with ω-CTx-GVIA, but especially motifs I and III, which are believed to occupy positions diametrically opposite each other across the pore mouth (Ellinor et al., 1994). These results suggest that the toxin straddles the external mouth of the pore while engaged in favorable interactions with residues in extracellular loops near the putative pore-forming region (e.g., IIIS5) (Ellinor et al., 1994). Furthermore, increases in external Ba^{2+} greatly slow ω-conotoxin block, consistent with the notion that the toxin comes close to divalent cations bound at the locus of selectivity (Boland et al., 1994; McDonough et al., 1996). Taken together, these observations suggest that the toxin interacts with the channel near the extracellular pore mouth, suggesting that this region harbors a conformational change associated with inactivation. This is reminiscent of the mechanism proposed for C-type inactivation in K^+ channels (Choi et al., 1991; López-Barneo et al., 1993; Yellen et al., 1994; Baukrowitz and Yellen, 1995, 1996).

An important aim for future experiments is to utilize the favorable properties of peptide toxins (rigid, well characterized backbone structure, many derivatives with extensively modified side chains) to obtain a clearer picture of the structural basis of inactivation. Residues near S6 segments, adjacent to the pore-forming region, are a logical place to start because they appear to be important in controlling the rate of voltage-dependent inactivation in Ca^{2+} channels such as *doe*-1 and α_{1A} (Zhang et al., 1994; Hering et al., 1996). Although toxin interactions can be most readily studied with the large collection of natural and synthetic ω-conotoxins known to affect N-type Ca^{2+} channels, any struc-

tural insights about inactivation are likely to apply across the entire family of voltage-gated Ca^{2+} channels.

REFERENCES

Aiyar J, Withka JM, Rizzi JP, Singleton DH, Andrews GC, Lin W, Boyd J, Hanson DC, Simon M, Dethlefs B, Lee C, Hall JE, Gutman GA, Chandy KG (1995) Topology of the pore-region of a K^+ channel revealed by the NMR-derived structures of scorpion toxins. Neuron 15:1169–1181.

Aosaki T, Kasai H (1989) Characterization of two kinds of high-voltage-activated Ca-channel currents in chick sensory neurons. Differential sensitivity to dihydropyridines and omega-conotoxin GVIA. Pflügers Arch 414:150–156.

Armstrong CM (1969) Inactivation of the potassium conductance and related phenomena caused by quaternary ammonium ion injection in squid axons. J Gen Physiol 54:553–575.

Armstrong CM (1971) Interaction of tetraethylammonium ion derivatives with the potassium channels of giant axons. J Gen Physiol 58:413–437.

Basus VJ, Nadasdi L, Ramachandran J, Miljanich GP (1995) Solution structure of ω-conotoxin MVIIA using 2D NMR spectroscopy. FEBS Lett 370:163–169.

Baukrowitz T, Yellen G (1995) Modulation of K^+ current by frequency and external $[K^+]$: a tale of two inactivation mechanisms. Neuron 15:951–960.

Baukrowitz T, Yellen G (1996) Use-dependent blockers and exit rate of the last ion from the multi-ion pore of a K^+ channel. Science 271:653–656.

Bean BP, Cohen CJ, Tsien RW (1983) Lidocaine block of cardiac sodium channels. J Gen Physiol 81:613–642.

Bean BP (1984) Nitrendipine block of cardiac calcium channels: high affinity binding to the inactivated state. Proc Natl Acad Sci USA 81:6388–6392.

Bezprozvanny I, Tsien RW (1995) Voltage-dependent blockade of diverse types of voltage-gated Ca^{2+} channels expressed in *Xenopus* oocytes by the Ca^{2+} channel antagonist mibefradil (Ro40-5967). Mol Pharmacol 48:540–549.

Bezprozvanny I, Scheller RH, Tsien RW (1995) Functional impact of syntaxin on gating of N-type and Q-type calcium channels. Nature 378:623–626.

Boland LM, Morrill JA, Bean BP (1994) ω-Conotoxin block of N-type calcium channels in frog and rat sympathetic neurons. J Neurosci 14:5011–5027.

Carbone E, Swandulla D (1990) Neuronal calcium channels: kinetics, blockade and modulation. Prog Biophys Mol Biol 54:31–58.

Catterall WA (1977) Membrane potential-dependent binding of scorpion toxin to the action potential Na^+ ionophore. J Biol Chem 23:8660–8668.

Catterall WA (1993) Structure and function of voltage-gated ion channels. Trends Neurosci 16:500–506.

Choi KL, Aldrich RW, Yellen G (1991) Tetraethylammonium blockade distinguishes two inactivation mechanisms in voltage-activated K^+ channels. Proc Natl Acad Sci USA 88:5092–5095.

Dunlap K, Luebke JI, Turner TJ (1995) Exocytotic Ca^{2+} channels in mammalian central neurons. Trends Neurosci 18:89–98.

Ellinor PT, Zhang J, Horne WA, Tsien RW (1994) Structural determinants of the blockade of N-type calcium channels by a peptide neurotoxin. Nature 372:272–275.

Farr-Jones S, Miljanich GP, Nadasdi L, Ramachandran J, Basus VJ (1995) Solution structure of ω-conotoxin MVIIC, a high affinity ligand of P-type calcium channels, using ^1H NMR spectroscopy and complete relaxation matrix analysis. J Mol Biol 248:106–124.

Feldman DH, Olivera BM, Yoshikami D (1987) Omega conus geographus toxin: a peptide that blocks calcium channels. FEBS Lett 214:295–300.

French RJ, Prusak-Sochaczewski E, Zamponi GW, Becker S, Kularatna AS, Horn R (1996) Interactions between a pore-blocking peptide and the voltage sensor of the sodium channel: an electrostatic approach to channel geometry. Neuron 16:407–413.

Fujita Y, Mynlieff M, Dirksen RT, Kim M-S, Niidome T, Nakai J, Friedrich T, Iwabe N, Miyata T, Furuichi T, Furutama D, Mikoshiba K, Mori Y, Beam KG (1993) Primary structure and functional expression of the omega-conotoxin-sensitive N-type calcium channel from rabbit brain. Neuron 10:585–598.

Hering S, Aczel S, Grabner M, Döring F, Berjukow S, Metterdorfer J, Sinnegger MJ, Striessnig J, Degitar VE, Wang Z, Glossmann H (1996) Transfer of high sensitivity for benzothiazepines from L-type to class A (BI) calcium channels. J Biol Chem 271:24471–24475.

Hidalgo P, MacKinnon R (1995) Revealing the architecture of a K^+ channel pore through mutant cycles with a peptide inhibitor. Science 268:307–310.

Hille B (1977) Local anesthetics: hydrophilic and hydrophobic pathways for the drug-receptor reaction. J Gen Physiol 69:496–515.

Hirning LD, Fox AP, McCleskey EW, Olivera BM, Thayer SA, Miller RJ, Tsien RW (1988) Dominant role of N-type Ca^{2+} channels in evoked release of norepinephrine from sympathetic neurons. Science 239:57–61.

Hondeghem LM, Katzung BG (1977) Time- and voltage-dependent interactions of antiarrhythmic drugs with cardiac sodium channels. Biochim Biophys Acta 472:373–398.

Hoshi T, Zagotta WN, Aldrich RW (1990) Biophysical and molecular mechanisms of Shaker potassium channel inactivation. Science 250:533–538.

Jones SW, Marks TN (1989) Calcium currents in bullfrog sympathetic neurons. J Gen Physiol 94:169–182.

Kasai H, Aosaki T, Fukuda J (1987) Presynaptic Ca-antagonist omega-conotoxin irreversibly blocks N-type Ca-channels in chick sensory neurons. Neurosci Res 4:228–235.

Komuro H, Rakic P (1992) Selective role of N-type calcium channels in neuronal migration. Science 257:806–809.

Larsson HP, Baker OS, Dhillon DS, Isacoff EY (1996) Transmembrane movement of the Shaker K^+ channel S4. Neuron 16:387–397.

Lee KS, Tsien RW (1983) Mechanism of calcium channel blockade by verapamil, D600, diltiazem and nitrendipine in single dialyzed heart cells. Nature 302:790–794.

Liu Y, Jurman ME, Yellen G (1996) Dynamic rearrangement of the outer mouth of a K^+ channel during gating. Neuron 16:859–867.

López-Barneo J, Hoshi T, Heinemann SH, Aldrich RW (1993) Effects of external cations and mutations in the pore region on C-type inactivation of *Shaker* potassium channels. Receptors and Channels 1:61–71.

McCleskey EW, Fox AP, Feldman D, Cruz LJ, Olivera BM, Tsien RW, Yoshikami D (1987) ω-Conotoxin: direct and persistent block of specific types of calcium channels in neurons but not muscle. Proc Natl Acad Sci USA 84:4327–4331.

McDonough SI, Swartz KJ, Mintz IM, Boland LM, Bean BP (1996) Inhibition of calcium channels in rat central and peripheral neurons by ω-conotoxin MVIIC. J Neurosci 16:2612–2623.

McEnery MW, Snowman AM, Sharp AH, Adams ME, Snyder SH (1991) Purified omega-conotoxin GVIA receptor of rat brain resembles a dihydropyridine-sensitive L-type calcium channel. Proc Natl Acad Sci USA 88:11095–11099.

Mintz I, Adams ME, Bean BP (1992) P-type calcium channels in rat central and peripheral neurons. Neuron 9:85–95.

Nemoto N, Kubo S, Yoshida T, Chino N, Kimura T, Sakakibara S, Kyogoku Y, Kobayashi Y (1995) Solution structure of ω-conotoxin MVIIC determined by NMR. Biochem Biophys Res Commun 207:695–700.

Nowycky MC, Fox AP, Tsien RW (1985) Three types of neuronal calcium channel with different calcium agonist sensitivity. Nature 316:440–443.

Pallaghy PK, Duggan BM, Pennington MW, Norton RS (1993) Three-dimensional structure in solution of the calcium channel blocker ω-conotoxin. J Mol Biol 234:405–420.

Pelzer D, Pelzer S, McDonald TF (1990) Properties and regulation of calcium channels in muscle cells. Rev Physiol Biochem Pharmacol 114:107–207.

Plummer MR, Logothetis DE, Hess P (1989) Elementary properties and pharmacological sensitivities of calcium channels in mammalian peripheral neurons. Neuron 2:1453–1463.

Randall AD, Tsien RW (1995) Pharmacological dissection of multiple types of Ca^{2+} channel currents in rat cerebellar granule neurons. J Neurosci 15:2995–3012.

Ranganathan R, Lewis JH, MacKinnon R (1996) Spatial localization of the K^+ channel selectivity filter by mutant cycle-based structure analysis. Neuron 16:131–139.

Regan LJ, Sah DWY, Bean BP (1991) Ca^{2+} channels in rat central and peripheral neurons: high-threshold current resistant to dihydropyridine blockers and ω-conotoxin. Neuron 6:269–280.

Ruth P, Rohrkasten A, Biel M, Bosse E, Regulla S, Meyer HE, Flockerzi

V, Hofmann F (1989) Primary structure of the beta subunit of the DHP-sensitive calcium channel from skeletal muscle. Science 245:1115–1118.

Sakamoto J, Campbell KP (1991) A monoclonal antibody to the beta subunit of the skeletal muscle dihydropyridine receptor immunoprecipitates the brain omega-conotoxin GVIA receptor. J Biol Chem 266:18914–18919.

Sather WA, Tanabe T, Zhang J-F, Mori Y, Adams ME, Tsien RW (1993) Distinctive biophysical and pharmacological properties of class A (BI) calcium channel α_1 subunits. Neuron 11:291–303.

Satin J, Limberis JT, Kyle JW, Rogart RB, Fozzard HA (1994) The saxitoxin/tetrodotoxin binding site on cloned rat brain IIa Na channels is in the transmembrane electric field. Biophys J 67:1007–1014.

Sevilla P, Bruix M, Santoro J, Gago F, Garcia AG, Rico M (1993) Three-dimensional structure of ω-conotoxin GVIA determined by ^{1}H NMR. Biochem Biophys Res Commun 192:1238–1244.

Stampe P, Kolmakova PL, Miller C (1994) Intimations of K^+ channel structure from a complete functional map of the molecular surface of charybdotoxin. Biochemistry 33:443–450.

Stanley EF, Goping G (1991) Characterization of a calcium current in a vertebrate cholinergic presynaptic nerve terminal. J Neurosci 11: 985–993.

Stühmer W, Conti F, Suzuki H, Wang X, Noda M, Yahagi V, Kubo H, Numa S (1989) Structural parts involved in activation and inactivation of the sodium channel. Nature 339:597–603.

Vassilev PM, Scheuer T, Catterall WA (1988) Identification of an intracellular peptide segment involved in sodium channel inactivation. Science 241:1658–1661.

Wheeler DB, Randall A, Tsien RW (1994) Roles of N-type and Q-type Ca^{2+} channels in supporting hippocampal synaptic transmission. Science 264:107–111.

Williams ME, Brust PF, Feldman DH, Patthi S, Simerson S, Maroufi A, McCue AF, Velicelebi G, Ellis SB, Harpold MM (1992) Structure and functional expression of an omega-conotoxin-sensitive human N-type calcium channel. Science 257:389–395.

Yang N, Horn R (1995) Evidence for voltage-dependent S4 movement in sodium channels. Neuron 15:213–218.

Yellen G, Sodickson D, Chen T-Y, Jurman ME (1994) An engineered cysteine in the external mouth of a K^+ channel allows inactivation to be modulated by metal binding. Biophys J 66:1068–1075.

Zagotta WN, Hoshi T, Aldrich RW (1990) Restoration of inactivation in mutants of *Shaker* potassium channels by peptide derived from ShB. Science 250:568–571.

Zhang J-F, Ellinor PT, Aldrich RW, Tsien RW (1994) Molecular determinants of voltage-dependent inactivation of calcium channels. Nature 372:97–100.